Macrophage ERα promoted invasion of endometrial cancer cell by mTOR/KIF5B –mediated epithelial to mesenchymal transition

Xuanxuan Jing¹, Jin Peng², Yu Dou¹, Jintang Sun¹, Chao Ma¹, Qingjie Wang¹, Lin

Zhang¹, Xia Luo², Beihua Kong², Yun Zhang¹, Lijie Wang²*, Xun Qu¹*

¹Institute of Basic Medical Sciences and Key Laboratory of Cardiovascular

Remodeling and Function Research, Qilu Hospital of Shandong University, Jinan,

Shandong, China

²Department of Obstetrics and Gynecology, Qilu Hospital of Shandong University,

Jinan, Shandong, China

*Corresponding author

Xun Qu, Institute of Basic Medical Sciences and Key Laboratory of Cardiovascular

Remodeling and Function Research, Qilu Hospital of Shandong University. 107 West

Wenhua Road, Jinan, 250012, Shandong, China. Phone: +8618560087979.

Fax:+8618560087979. email: quxun@sdu.edu.cn.

This article has been accepted for publication and undergone full peer review but has not been through the copyediting, typesetting, pagination and proofreading process, which may lead to differences between this version and the Version of Record. Please cite this article as doi: 10.1111/imcb.12245

Lijie Wang. Department of Obstetrics and Gynecology, Qilu Hospital of Shandong University. 107 West Wenhua Road, Jinan, 250012, Shandong, China. Phone: +8618560081857. Fax:+8618560081857. email: wangljie@hotmail.com

Running Title: Macrophage ER induce EMT of endometrial tumor cell

Key words: CCL18, Estrogen receptor α, Endometrial cancer, KIF5B, Macrophage

Abstract

Tumor associated macrophages (TAMs) exert tumor-promoting effects. There have been reports that Estrogen receptors (ERs) are expressed on the infiltrating macrophages of endometriosis, ovarian cancer and lung cancer. However, the role of ERs in macrophages is not well characterized. In this study, we first identified that ERα expression on the macrophages of human endometrial cancer was positively correlated with cancer progression. Conditioned medium from selective ERα agonist-treated M2 macrophages induced the epithelial to mesenchymal transition (EMT) in endometrial cancer cells. However, this effect can be inhibited by ERα antagonist. Here, we showed that macrophages ERα-engaged abundantly produced CCL18, and its expression promoted the invasion of endometrial cancer cells by

activating the ERK1/2 pathway, whereas suppressing CCL18 abrogated these effects. Furthermore, we initially identified that CCL18 derived from TAMs upregulated KIF5B expression to promote EMT via activating the PI3K/AKT/mTOR signaling pathway in endometrial cancer. Overall, our findings show how ERα-engaged infiltrating macrophages initiate chronic inflammation and promote the aggressive progression of endometrial cancer cells. ERα-positive TAMs act as drivers of endometrial cancer, which may become a potential therapeutic target.

INTRODUCTION

Recent studies of endometrial cancer have revealed that chronic inflammation participates in tissue remodeling of the tumor microenvironment, thus promoting tumor growth, invasion and angiogenesis. The periodic damage and repair process of the endometrium is regarded as chronic inflammation response. Consequently, the obvious and persistent inflammatory microenvironment in endometrial cancer plays decisive roles in tumor progression. Tumor associated macrophages (TAMs) account for about 50% of the immune cells infiltrated within tumor microenvironment. Macrophages are derived from monocytes and exhibit two distinct phenotypes: M1 (activated by IFN-r and LPS) and M2 phenotype (stimulated by IL-4 and IL-13). M1 macrophages predominantly play roles in antigen presentation and killing of pathogenic microorganisms, while the M2 phenotype exerts pro-tumoral

effects. TAMs participate in tumor progression via the secretion of an array of cytokines, chemokines and growth factors. 6-8 Currently, it remains unclear how TAMs play roles in endometrial cancer progression.

CCL18 is predominantly secreted by M2 macrophages. The upregulation of CCL18 in M2 macrophages has been discovered in several inflammatory diseases. In addition, CCL18 overexpression has been observed in the macrophages of several tumors, including ovarian cancer, gastric cancer and glioma. Furthermore, CCL18 promotes the epithelial mesenchymal transition (EMT) mediated-metastasis in breast cancer. 9-12

Epithelial properties can transform into mesenchymal phenotypes, allowing the epithelium to acquire motile and invasive behaviors, which is named as EMT.^{13,14} Substantial evidence verifies that kinesin superfamily (KIF) participates in the development of cancers.¹⁵ KIFs are involved in functions related to cellular motility, such as the transport of macromolecules. There are three subtypes of KIF5, including KIF5A, KIF5B, and KIF5C. KIF5 is also involved in the transport of mitochondria.¹⁶

The PI3K/AKT/mTOR signaling pathway is overactivated in many tumors and participates in cancer invasion.¹⁷ The mTOR is a large serine/threonine protein kinase, including two distinct complexes: mTORC1 and mTORC2. The inhibition of mTOR

has been used as first-line therapy for advanced stage ovarian cancer patients in clinical trial. 18

Recent discoveries have identified that estrogen plays a potential immunoregulatory role in the tumor microenvironment.¹⁹ There are two classical estrogen receptor subtypes, namely, ERα and ERβ. Reports have indicated that estrogen induces the polarization and infiltration of M2 macrophages in breast cancer.²⁰ Estrogen stimulates tumor cell proliferation by promoting M2 macrophage secretion of IL-17A in endometrial cancer.²¹ However, it is not clear whether the effect of macrophages on endometrial cancer occurs through the modulation of ERs.

Numerous studies have revealed that tumor cells interact with stromal cells within microenvironment and initiate tumorigenesis. We hypothesize that estrogen may interact with macrophages to participate in the development of endometrial cancer. In this research, we study the effect of ER α positive macrophages on the development of endometrial cancer and further investigate the underlying molecular mechanism.

RESULTS

The number of $\text{ER}\alpha^+$ macrophages in tumoral tissue correlates with the clinical stage of endometrial cancer

CD68-positive macrophages were detected in 56 out of the 85 (65.8%) endometrial cancer specimens. The mean number of CD68⁺ macrophages in endometrial cancer tissue was higher than that in normal tissue (P < 0.001, Figure 1a). CD68⁺ macrophages in tumor specimens were classified into three groups: nest macrophages, stroma macrophages and margin macrophages (Figure 1b). The density of stroma or margin CD68⁺ macrophages was remarkably higher than that of nest macrophages (P < 0.001, P < 0.001, respectively). There was no difference in the CD68⁺ macrophage density between the stroma group and the margin group (P > 0.05, Figure 1c). Furthermore, we found out the number of CD68⁺ macrophages in the tumoral stroma was correlated with lymph node metastasis and FIGO stage of endometrial cancer (Table 1).

Because endometrial cancer is an estrogen-related tumor, we estimated $ER\alpha$ expression in the epithelial and stromal compartments of endometrial cancer. The $ER\alpha$ expression score of the epithelial and stromal compartments was lower in the advanced stage (stage 3-4) group than in the early stage (stage 1-2) group. This result implies a negative association between $ER\alpha$ expression in the epithelial and stromal

compartments and the FIGO stage of endometrial cancer (P < 0.001, Figure 1d). In addition, we found that ER α was expressed on the macrophages of endometrial cancer tissue (Figure 1f; Supplementary figures 1a, b). The tissue with ER α ⁺CD68⁺ macrophages accounted for 46.4% of those with CD68⁺ macrophages in tumor specimens, and only 21.4% of those in normal tissues (P < 0.05, Figure 1e). Unexpectedly, the percentage of tissues with ER α ⁺CD68⁺ macrophages in the advanced stage group (73.9%) was notably higher than that in the early stage group (27.3%) (P < 0.01, Figure 1g). These data implied that ER α ⁺ macrophages in endometrial cancer were positively correlated with the progression of endometrial cancer.

M2 macrophages treated with ER α agonist induced EMT in endometrial cancer cells via CCL18

To verify that ERα on macrophages are involved in the progression of endometrial cancer, we performed an array of *in vitro* assays. When treated with CM from ERα agonist (PPT)-stimulated M2 cells (M2-PPT-CM), the number of migrating Ishikawa cells increased almost 2-fold compared with the control, while the effect of PPT was counteracted by the ERα antagonist (MPP) in Ishikawa cells (Figures 2a, b). The results of the wound healing assay were in accordance with those of the Transwell assay (Figures 2c, d). A 3D invasion assay was performed to examine the effect of

M2-PPT-CM on the invasion of endometrial cancer cells. Ishikawa cells cultured with M2-PPT-CM formed longer invasive projections compared with control cells. Similarly, MPP reversed the effect of PPT on invasion (Figures 2e, f). To confirm these findings, we investigated the effect of M2-PPT-CM on the characterization of cell morphology and the microtubule and actin cytoskeleton. Compared with the control, the cell morphology of Ishikawa treated with M2-PPT-CM appeared irregular and longer, and the microtubule and actin cytoskeleton appeared more organized and had directionality, indicating that microtubules may be more dynamic. Blocking ERa with MPP, the actin cytoskeleton and microtubules appeared less organized, and the irregular cell morphology change was reversed (Figure 2g). The expression of EMT markers was examined by Western blotting and qRT-PCR, and the expression of the epithelial marker (E-cadherin) in Ishikawa treated by M2-PPT-CM were significantly decreased, while mesenchymal markers (N-cadherin, Vimentin) and transcription factor Twist1 were significantly upregulated. The effect of M2-PPT-CM on EMT markers expression could be partially reversed by blocking ERα with MPP (Figures 2h-j). Thus, the CM from ERα agonist-treated M2 macrophages induced EMT and promoted the migration and invasion of endometrial cancer cells.

Previous studies have shown the relationship between CCL family members and EMT in various tumors. Then, we investigated the $ER\alpha$ -mediated chemokine and cytokine profiles in M2 macrophages. The mRNA level of CCL18 increased nearly 12-fold in This article is protected by copyright. All rights reserved.

the PPT-treated group compared with that in the control and blocking ERα with MPP reversed the PPT-induced CCL18 upregulation (Figure 3a). To confirm the above data, we performed ELISA to examine the CM from PPT- or MPP-treated M2 cells. The secretion of CCL18 protein in the PPT-treated group significantly increased nearly 2-fold compared with the control, and MPP inhibited PPT-induced CCL18 upregulation (Figure 3b). However, the mRNA and protein levels of IL-1β, IL-6, IL-10, IL-12 and MCP-1 were not affected by the CM from PPT or MPP-treated M2 cells (Figures 3a, b).

In addition, we investigated the molecular mechanism underlying the ERα agonist-induced CCL18 secretion in M2 macrophages. We found that PPT increased the p-ERK1/2 protein levels of M2 macrophages in a time-dependent manner and the activation peaked at 2 h after PPT treatment. However, there was no influence on the total ERK1/2 protein levels of M2 macrophages incubated with PPT (Figures 3c, d). PPT-induced ERK1/2 phosphorylation was reversed by MPP, indicating that the activation of p-ERK1/2 was dependent on ERα (Figures 3e, f). Moreover, the inhibitor of ERK1/2 remarkably counteracted PPT-induced CCL18 secretion (Figure 3g). The above data suggested that the ERα agonist induced CCL18 secretion by activating the ERK1/2 pathway.

Then, we identified the effect of CCL18 secreted by TAMs on the progression of endometrial cancer. Treatment with recombinant CCL18 (rCCL18) for 12 h promoted the migration and invasion of Ishikawa cells in a dose-dependent manner (Figures 4a-f). The morphology of Ishikawa cells incubated with rCCL18 appeared irregular and longer, and the microtubule and actin cytoskeleton appeared more organized and had directionality (Figure 4g). These changes of morphology are consistent with the EMT. The expression of E-cadherin in Ishikawa cells treated with rCCL18 significantly decreased and N-cadherin, Vimentin and Twist1 were significantly upregulated in a dose dependent manner compared with the control (Figures 4h-j). Therefore, rCCL18 induced the EMT in endometrial cancer cells.

We further investigated whether CCL18 was involved in ERα agonist-treated M2-induced EMT in endometrial cancer cells. An anti-CCL18 antibody was employed to neutralize the effect of CCL18 in M2-PPT-CM. We found that the effect of M2-PPT-CM on the migration and invasion of Ishikawa was abrogated by the anti-CCL18 antibody (Figures 2a-f). Furthermore, the changes of cell morphology and microtubule and actin cytoskeleton status induced by M2-PPT-CM were also reversed by CCL18 antibody (Figure 2g). The expression change of EMT markers induced by M2-PPT-CM was also counteracted by the CCL18 neutralizing antibody (Figures 2h-j). Similarly, M2-PPT-CM also induced the EMT in KLE cells by CCL18 secretion, which was in accordance with that in Ishikawa (Supplementary figures 2a-h). We also

treated endometrial cancer cells with ER α -agonist or antagonist directly, and the data showed that ER α -agonist or antagonist did not affect the expression of EMT markers in Ishikawa and KLE cells (Supplementary figures 3a, b), indicating that ER α -agonist or antagonist has no direct effect on the EMT of endometrial cancer cells. Here, we first identified that ER α agonist-treated M2 induced the EMT of endometrial cancer cells via CCL18.

Human peripheral blood monocytes-derived M2 macrophages treated with ERα agonist induced EMT in endometrial cancer cell Ishikawa

ERα was also expressed on human peripheral blood monocytes (PBMC)-derived macrophages (Supplementary figures 4a, b). ERα agonist could stimulate the secretion of CCL18 in PBMC-derived M2 macrophages. PBMC-derived macrophages treated with ERα agonist induced EMT and promoted the migration of Ishikawa cells and the effect was reversed by anti-CCL18 neutralization antibody, which was in accordance with the results that used the CM of THP1-derived M2 macrophages (Supplementary figures 4c-g).

rCCL18 and CCL18 from ERα agonist-treated M2-CM induced the EMT of Ishikawa cells via KIF5B

KIFs play important roles in tumor migration and invasion. However, the roles of KIFs in the progression of endometrial cancer are not well characterized. We investigated whether CCL18 induced EMT in Ishikawa cells via KIFs. Treatment of Ishikawa cells with rCCL18 for 24 h dramatically increased the mRNA level of KIF5B in a dose-dependent manner. However, the expression of KIF1B, KIF3A and KIF3B was not affected by rCCL18 (Figure 5a). Treatment of Ishikawa cells with M2-PPT-CM also increased KIF5B mRNA levels compared with the control. However, this effect could be inhibited by CCL18 neutralizing antibody (Figure 5b). To validate whether rCCL18 or M2-PPT-CM induced EMT by KIF5B, we constructed KIF5B-siRNA. M2-PPT-CM or rCCL18 did not influence the migration of Ishikawa cells transfected with KIF5B-siRNA (Figures 5c-f). The effect of M2-PPT-CM or rCCL18 on cell morphology and microtubule and actin cytoskeleton was diminished in Ishikawa cells transfected with KIF5B-siRNA (Figures 5g, h). Furthermore, KIF5B knockdown influenced the expression of EMT markers. The expression of E-cadherin was increased and N-cadherin, Vimentin and Twist1 were significantly decreased in Ishikawa cells transfected with KIF5B-siRNA compared with the control (Figures 5i-k). Here, we first revealed the relationship between KIF5B and EMT. Collectively, the above data suggested that CCL18 from M2-PPT-CM induced EMT in Ishikawa cells by KIF5B.

Immunohistochemistry was performed to investigate the effect of KIF5B on the progression of endometrial cancer. KIF5B was predominantly expressed in the epithelial compartment of endometrial cancer tissue (Figure 6a). All of the cases were classified into KIF5B^{high} and KIF5B^{low} expression groups. Approximately 94% of endometrial tumor specimens were considered as highly expressing KIF5B, while only 69% in normal tissue. KIF5B expression in tumor tissue was significantly higher than that in normal tissue (P < 0.001, Figure 6b). Furthermore, the KIF5B staining intensity of tumor tissue was positively correlated with the FIGO stage (P < 0.01, Table 2). The number of CD68⁺ macrophages was positively correlated with KIF5B expression scores in the epithelial compartment of endometrial cancer (r = 0.442, P < 0.001. Figure 6c). These results indicated that CD68⁺ macrophage infiltration was correlated with KIF5B expression in the epithelial compartment of endometrial cancer.

 $ER\alpha$ agonist-treated M2 cells induced EMT in Ishikawa cells through the PI3K/AKT/mTOR signaling pathway

To identify the underlying signaling pathway of Ishikawa cells treated with rCCL18 or M2-PPT-CM, we measured the protein phosphorylation level of the PI3K/AKT/mTOR signaling pathway. The p-AKT and p-mTOR protein levels in Ishikawa cells cultured with rCCL18 for 2 h were upregulated in a dose-dependent manner (Supplementary figures 5a, c). Similarly, the treatment of Ishikawa cells with

M2-PPT-CM also increased p-AKT and p-mTOR protein levels compared with the control. However, the effect was inhibited by 10 ug mL⁻¹ CCL18 neutralizing antibody (Supplementary figures 5b, d). The protein levels of PI3K, AKT and mTOR in Ishikawa cells were not affected by rCCL18 or M2-PPT-CM. To further verify whether the excessive activation of the PI3K/AKT/mTOR pathway was related to M2-PPT-CM-induced KIF5B upregulation and EMT in Ishikawa cells, an mTOR inhibitor INK128 was employed. The mTOR inhibitor significantly counteracted KIF5B upregulation induced by rCCL18 or M2-PPT-CM (Supplementary figures 5e, f). In addition, the effect of rCCL18 or M2-PPT-CM on the migration of Ishikawa cells was also inhibited by the mTOR inhibitor (Supplementary figures 5g-j). In conclusion, these data indicated that rCCL18 or M2-PPT-CM induced KIF5B upregulation and EMT in Ishikawa cells by activating the PI3K/AKT/mTOR signaling pathway.

DISCUSSION

In our study, the CD68⁺ macrophage density was significantly higher in endometrial cancer specimens than counterparts, which was consistent with a previous study.²³ Macrophages are the main immune cells in the endometrium and exert multiple biological effects following the menstrual cycle.²⁴ Similar to a previous study,²⁵ our data showed that the TAM density in endometrial cancer was significantly related to

tumor clinical stage and lymph node metastasis. Because endometrial cancer is an estrogen-related tumor, we unexpectedly discover a negative association between ER α expression in the epithelial and stromal compartment and the FIGO stage of endometrial cancer. At present, researches on ER α expression and endometrial cancer progression have inconsistent conclusions. ^{26,27} One previous report indicated epithelial ER α expression was negatively correlated with FIGO stage of endometrial cancer. ²⁸

In recent years, the effect of estrogen on tumor microenvironment has attracted the attention of many researchers. ¹⁹ Studies have indicated that ERs are expressed on the TAMs of ovarian cancer. ²⁹ ER β is expressed on the TAMs of murine lung cancer. ³⁰ Furthermore, the human monocyte cell line THP1 and human PBMC-derived macrophages express ER α , which are in line with previous reports. ³¹⁻³⁴ Our data are the first to validate the expression of ER α on partial of CD68⁺ macrophages in endometrial cancer. Interestingly, ER α ⁺ macrophages in endometrial cancer are significantly correlated with endometrial cancer progression.

In view of the limited number of $ER\alpha^+$ macrophages in tumor stroma, we examined its influence on endometrial cancer cell migration and invasion. We verified that $ER\alpha$ agonist-treated THP1 or PBMC derived-M2 induced EMT in endometrial cancer cells Ishikawa and KLE, which was reversed by an $ER\alpha$ antagonist. In conclusion, our data

verified $\text{ER}\alpha$ in macrophages mediated the effect of neoplastic metastasis in endometrial cancer.

Macrophages account for about 50% of the tumor stroma, and these cells promote invasion via remolding the nearby environment. Fibroblast ER α induces CCL1 secretion and promotes bladder cancer cell invasion. CCL18 is correlated with tumor progression and prognosis in ovarian, endometrial, and breast cancers. However, studies about the effect of CCL18 on cancer development have controversial conclusions. In gastric cancer, high CCL18 levels predicts better prognosis We first identified that ER α agonist-treated M2 induced EMT of endometrial cancer cells via CCL18. Furthermore, we validated that ER α agonist enhanced CCL18 secretion by the ERK1/2 pathway in M2.

Interestingly, our immunohistochemistry results indicated that KIF5B expression in tumor tissue was higher than counterparts and was positively correlated with the clinical stage of endometrial cancer. KIFs participate in various physiological activities related to celluar motility. Substantial evidence verifies that KIFs participate in the malignant biological behavior of cancers. KIF2A and KIF2C are overexpressed in immortalized human bronchial epithelial cells, subsequently promote EMT in cancer cells. KIF5B upregulation is discovered in several cancers.

present study, we first identified that KIF5B participated in the EMT in endometrial cancer cells. Moreover, rCCL18 and ERα agonist-treated M2 cells upregulated KIF5B expression in Ishikawa cells, which mediated the status of the microtubule and actin cytoskeleton and made microtubules be more dynamic, thus promoting the invasion of endometrial cancer cells. However, KIF5B knockdown abrogated the effect of rCCL18 or ERα agonist-treated M2 upon EMT induction. We first verified the role of KIF5B in endometrial cancer and showed that ERα agonist-treated M2 promoted EMT in endometrial cancer cells by KIF5B.

The PI3K/AKT/mTOR pathway is overactivated in various tumors, which contributes to neoplastic metastasis. Research has indicated that CCL18 in the oral carcinoma microenvironment induces EMT via the mTOR pathway. Herthermore, inhibiting mTORC2 could reverse EMT and inhibit the movement of cancer cells in renal cell carcinomas. Furthermore, in prostate cancer, inhibiting mTOR by INK128 could decrease the invasion of cancer cells via Vimentin and Twist downregulation. Our data showed that rCCL18 and ERα agonist-treated M2 cells promoted the phosphorylation of AKT and mTOR and CCL18-induced KIF5B upregulation and migration enhancement were partially inhibited by mTOR inhibitor INK128. Therefore, CCL18 secreted by TAMs in the tumor microenvironment upregulated KIF5B expression, thus promoting EMT and neoplastic metastasis by the PI3K/AKT/mTOR signaling pathway in endometrial cancer (Supplementary figure 6).

METHODS

Reagents and antibodies

ERα-selective agonist (PPT) and ERα-selective antagonist (MPP) were purchased from Sigma (St Louis, MO, USA). The recombinant CCL18, anti-CCL18 neutralizing antibody and ELISA kits were purchased from R&D (Minneapolis, MN, USA). The Matrigel was from BD (San Diego, CA, USA). INK128 was from MCE (Monmouth, NJ, USA). All the antibodies used in Western blotting were purchased from CST (Boston, MA, USA). The mouse anti-CD68 antibody was from abcam (Cambridge, UK) and mouse anti-ERα antibody was from Santa Cruz (CA, USA)

Clinical samples and immunohistochemistry

The tissue microarray (TMA) containing 85 endometrial cancer cases was obtained from Shanghai Outdo Biotech Company (Shanghai, China). The histopathologic characteristics include FIGO stage, grade, tumor type and growth pattern. Tissue arrays was deparaffinized in xylene and rehydrated in an ethanol gradient. Tissues were incubated with anti-CD68 (1:200) and ERα (1:200) overnight at 4°C and then incubated with secondary antibodies for 1 h at 37°C. The cover slips were mounted and evaluated for positive staining. Furthermore, double immunohistochemistry staining (CD68 and ERα) was also performed according to the instruction of Polymer

staining kits (DS-0001, Zhongshan, China). The slides were incubated with DAB and GBI-Permanent Red, and then counterstained with hematoxylin.

CD68, ERa and KIF5B evaluation

Blinded review was performed independently by two pathologists. For CD68 evaluation in TMA, we counted the numbers of CD68⁺ cells in 5 random fields at 400× magnification in each tissue core. CD68⁺ macrophages in tumor specimens were stratified into nest macrophages, stroma macrophages and margin macrophages. ⁴⁴ For double staining, CD68 was stained with yellow and ERα was stained with red. KIF5B and ERα expression were evaluated by counting the percentage of positive cells and scored the staining intensity. ⁴⁵

Cells culture

The human endometrial cancer cell line Ishikawa was kindly provided by the Department of Pathology, Shandong University. The human endometrial cancer cell line KLE was kindly provided by Shandong Provincial Hospital. The human monocyte line THP1 was obtained from ATCC. All cells were cultured in phenol red-free RPMI 1640 supplemented with 10% Charcoal Stripped fetal bovine serum (FBS) at 37°C, 5% CO₂. To generate M2 macrophages, THP-1 (1×10⁶ cells/well) was treated with 100 ng

mL⁻¹ PMA for 6 h and then cultured with PMA plus IL-4 (20 ng mL⁻¹) and IL-13 (20 ng mL⁻¹) for another 42 h. Then all PMA, IL-4 and IL-13 were removed by a thorough wash.⁴⁶ The expression of M2 markers in THP1-derived M2 macrophages is shown in Supplementary figure 7a. M2 cells were incubated in the presence of 10 nM PPT for 24 h. The cells were also untreated or pretreated with 10 nM MPP for 30 min.⁴⁷ DMSO was used as a control. Then, PPT, MPP or DMSO were removed by a thorough washing. M2 cells were further cultured in 2 ml fresh medium for another 24 h. CM were collected respectively.

Preparation and isolation of PBMC

We isolated human peripheral blood monocytes (PBMC) from three donors using Ficoll-Hypaque and anti-CD14 microbeads. To generate M2 macrophages, mononuclear cells were treated with 100 ng mL⁻¹ M-CSF for 5 days and then cultured with IL-4 (20 ng mL⁻¹) and IL-13 (20 ng mL⁻¹) for another 3 days. To generate M1 macrophages, mononuclear cells were treated with 50 ng mL⁻¹ GM-CSF for 5 days and then cultured with LPS (100 ng mL⁻¹) and IFN-r (20 ng mL⁻¹) for another 3 days. The expression of M2 markers in PBMC-derived M2 macrophages is shown in Supplementary figure 7b. This study has been approved by the institutional review board of Qilu Hospital of Shandong University. Informed consent was obtained from each subject.

Immunofluorescence of PBMC-derived M2 macrophages

Macrophages were stained with anti-CD68 (1:100) and ERα (1:50) overnight at 4°C. The cells were incubated with secondary antibodies Alexa Fluor 488 (green fluorescence). Nuclei was stained with DAPI (blue fluorescence). The cells were viewed using Olympus fluorescence microscopy.

3D invasion assay

To generate 3D tumor spheroid formation, 5×10^3 Ishikawa cells were added to a 24-well low attachment surface plate. After 3-4 days later, compacted spheriods were collected. Then Ishikawa spheroids were resuspended with Matrigel and evenly spread in 24-well plates. After the Matrigel solidified, M2-PPT-CM or rCCL18 was added to the top of the Matrigel to provide a chemogradient for the spheroids. M2-DMSO-CM or PBS were used as controls. We photographed the spheroid every days for a week. Then the longest distance of invasion was quantified with Image J from 3 random fields (200×) for every group.

Cytoskeleton staining assay

Ishikawa cells were seeded onto glass slides and cultured with M2-PPT-CM or rCCL18. M2-DMSO-CM or PBS was used as a control. After 48 h, the cells were fixed with 4% paraformaldehyde for 30 min, and permeabilized with 0.1% Triton X-100 for 5 min. The cells were stained with anti-α-tubulin antibody overnight at 4°C. F-actin and nuclei were stained with CytoPainter Phalloidin-iFluor 488 reagent and DAPI nuclear stain, respectively. The slides were viewed using Olympus confocal microscopy.

Enzymes linked immunosorbent assay (ELISA)

Cytokine or chemokine levels in M2-DMSO-CM, M2-PPT-CM and M2-MPP+PPT-CM were measured using human ELISA kits in accordance with the manufacturer's instructions.

Quantitative real-time PCR

RNA was extracted using Trizol. Reverse transcriptase reactions was performed using a qPCR RT kit. qRT-PCR was performed using SYBR Green on the LightCycler 2.0 instrument. GAPDH was used as control. The primer sequences are diaplayed in Supplementary table 1.

Western blotting

Total protein was lysed with RIPA buffer containing 1% PMSF and then separated by electrophoresis and then blotted onto PVDF membranes, then incubated with primary antibody overnight at 4°C, and then incubated with secondary antibodies. Finally, immunoreactivity was detected by an ECL detection kit.

Construction of KIF5B-siRNAs

KIF5B-siRNA was synthesized with the following sequences: siKIF5B-1: 5'-GGACCUGGCUACAAGAGUUTT-3' and siKIF5B-2: 5'-AACUCUUGUAGC CAGGUCCTT-3'. A nonspecific shRNA was used as a negative control. Ishikawa cells (3×10⁵/well) were plated onto 6-well plates. When the cells reached 70% confluence, KIF5B-siRNA with Lipofectamine 2000 was transfected into the cells for 48 h.

Statistical analysis

All statistical analyses were performed by using SPSS 13.0. All experiments were performed three times, and data were presented as the mean \pm SEM. Student's t test or Mann-Whitney U-test and ANOVA were used for statistical comparisons. Nonparametric Spearman's correlation was used to analyze the correlation between

two variables and chi-square test or Fisher's exact test were used to determine the differences in clinicopathological parameters between different groups. P < 0.05 was considered statistically significant.

SUPPORTING INFORMATION

Supplementary table 1. Primer sequences used in qRT-PCR

Supplementary figure 1. Immunohistochemical double staining of CD68/ER α in endometrial tumor specimens. (**a, b**) Shown were two representative sections (400×). Scale bar: 20µm. CD68 was stained with yellow and ER α was stained with red. ER α +CD68+ macrophage was shown by green arrow and ER α -CD68+ macrophage was shown by black arrow.

Supplementary figure 2. ERα agonist-treated M2 cells induced EMT of KLE cells by CCL18 secretion. (a) Transwell chamber assay of KLE cells incubated in CM from 10 nM PPT or MPP treated-M2 cells with or without 10 μg mL⁻¹ anti-CCL18 antibody for 12 h. (b) Analysis of the mean counts of migrating cells per field. (mean+SEM, ANOVA, 3 independent experiments). (c) Wound healing assay of KLE cells treated the same as (a) for 24 h. (d) Quantification of wound recovery. (mean+SEM, ANOVA, 3 independent experiments). (e) Typical images of 3D spheroid of KLE cells treated

the same as (a) for 72 h. (f) Quantification of the longest invasion distance (fold change). (mean+SEM, ANOVA, 3 independent experiments). (g) Representative morphology images from 3 independent experiments of KLE cells treated the same as (a) for 48 h in bright field. (h) The mRNA level of EMT markers in KLE cells treated as described above. (mean+SEM, ANOVA, 3 independent experiments). Scale bar: 20 μ m. *P < 0.05, **P < 0.01, ***P < 0.001.

Supplementary figure 3. The ERα agonist had no direct effect on the EMT markers in endometrial cancer cells. The mRNA level of EMT markers in (a) Ishikawa and (b) KLE cells treated with 10 nM PPT or MPP. (mean+SEM, ANOVA, 3 independent experiments).

Supplementary figure 4. ERα agonist-treated PBMC-derived M2 cells induced EMT in Ishikawa cells. (a) Representative immunofluorescence staining from 3 independent experiments of CD68 and ERα in human PBMC-derived M2 macrophages. (400×). Scale bar: 20 μm. (b) Typical images of M2 macrophages derived from PBMC in bright field. (c) The mRNA level of EMT markers in Ishikawa cells treated with CM from 10 nM PPT or MPP treated-PBMC-derived M2 macrophages with or without 10 μg mL⁻¹ anti-CCL18 antibody for 24 h. (mean+SEM, ANOVA, 3 independent experiments). (d) Transwell assay of Ishikawa cells treated the same as (c) for 12 h. (e)

Analysis of the mean counts of migrating cells per field. (mean+SEM, ANOVA, 3 independent experiments). (**f**) Wound healing assay of Ishikawa cells treated the same as (**c**) for 24 h. (**g**) Quantification of wound recovery. (mean+SEM, ANOVA, 3 independent experiments). (**h**) Representative morphology images from 3 independent experiments of Ishikawa cells treated the same as (**c**) for 48 h in bright field. Scale bar: $20 \, \mu \text{m}$. *P < 0.05, **P < 0.01, ***P < 0.001.

Supplementary figure 5. CM from ER α agonist-treated M2 cells or rCCL18 promoted KIF5B expression and the migration of Ishikawa cells via the PI3K/AKT/mTOR pathway (a, b) Representative western blotting from 3 independent experiments of the phosphorylation level of the PI3K/AKT/mTOR pathway in Ishikawa cells treated with rCCL18 (10 ng mL⁻¹ and 20 ng mL⁻¹) or M2-PPT-CM in the presence or absence of anti-CCL18 at 10 µg mL⁻¹ for 2 h. (c, d) Bar graphs representing the relative protein expression (fold change). (mean+SEM, ANOVA). (e, f) The mRNA levels of KIFs in Ishikawa cells treated with 20 ng mL⁻¹ rCCL18 or M2-PPT-CM in the presence or absence of INK128 (an mTOR inhibitor, 100 nM) for 24 h. (mean+SEM, ANOVA, 3 independent experiments). (g-j) Typical images and quantification of Transwell assay in Ishikawa cells incubated with 20 ng mL⁻¹ rCCL18 or M2-PPT-CM in the presence or absence of INK128 (100 nM) for 12 h. (mean+SEM, ANOVA, 3 independent experiments). Scale bar: 20 μm. *P < 0.05, **P < 0.01, ***P < 0.001.

Supplementary figure 6. The summary diagram exhibiting the interactions between macrophages $ER\alpha$ and endometrial cancer cells. CCL18 secreted by macrophages activated the PI3K/AKT/mTOR signaling pathway, which upregulates KIF5B expression, thus promoting EMT and the migration and invasion of endometrial cancer cells.

Supplementary figure 7. The expression of M2 markers in THP1 or human PBMC-derived M2 macrophages. The mRNA level of CD163, CD206 and IL-10 were increased in (a) THP1 or (b) PBMC-derived M2 macrophages compared with M1, and the transcription of IL-6 was increased in THP1 or human PBMC-derived M1 macrophages compared with M2. (mean+SEM, *P < 0.05, **P < 0.01, ***P < 0.001, *P < 0.001, *P = 0.0

ACKNOWLEDGMENTS

This work was supported by National Key Research and Development Program of China (2018YFC1002803), National Natural Science Foundation of China (No. 31470885, No. 81772879, No. 31300752). We thank Qianqian Shao for assistance with chart production.

CONFLICT OF INTEREST

The authors have nothing to disclose.

REFERENCES

- 1. Dossus L, Lukanova A, Rinaldi S, *et al.* Hormonal, metabolic, and inflammatory profiles and endometrial cancer risk within the EPIC cohort--a factor analysis. *Am J Epidemiol* 2013; **177**: 787-799.
- 2. Grivennikov SI, Greten FR, Karin M. Immunity, inflammation, and cancer.

 Cell 2010; 140: 883-899.
- 3. Evans J, Salamonsen LA. Decidualized human endometrial stromal cells are sensors of hormone withdrawal in the menstrual inflammatory cascade. *Biol Reprod* 2014; **90**: 14.
- 4. Graziottin A, Zanello PP. [Menstruation, inflammation and comorbidities: implications for woman health]. *Minerva Ginecol* 2015; **67**: 21-34.
- 5. Suarez-Carmona M, Lesage J, Cataldo D, *et al.* EMT and inflammation: inseparable actors of cancer progression. *Mol Oncol* 2017; **11**: 805-823.
- 6. Gajewski TF, Schreiber H, Fu YX. Innate and adaptive immune cells in the tumor microenvironment. *Nat Immunol* 2013; **14**: 1014-1022.

- 7. Noy R, Pollard JW. Tumor-associated macrophages: from mechanisms to therapy. *Immunity* 2014; **41**: 49-61.
- 8. Solinas G, Germano G, Mantovani A, *et al.* Tumor-associated macrophages (TAM) as major players of the cancer-related inflammation. *J Leukoc Biol* 2009; **86**: 1065-1073.
- 9. Chen J, Yao Y, Gong C, et al. CCL18 from tumor-associated macrophages promotes breast cancer metastasis via PITPNM3. Cancer Cell 2011; 19: 541-555.
- 10. Chang CY, Lee YH, Leu SJ, *et al.* CC-chemokine ligand 18/pulmonary activation-regulated chemokine expression in the CNS with special reference to traumatic brain injuries and neoplastic disorders. *Neuroscience* 2010; **165**: 1233-1243.
- 11. Schutyser E, Struyf S, Proost P, *et al.* Identification of biologically active chemokine isoforms from ascitic fluid and elevated levels of CCL18/pulmonary and activation-regulated chemokine in ovarian carcinoma. *J Biol Chem* 2002; 277: 24584-24593.
- Zohny SF, Fayed ST. Clinical utility of circulating matrix metalloproteinase-7
 (MMP-7), CC chemokine ligand 18 (CCL18) and CC chemokine ligand 11
 (CCL11) as markers for diagnosis of epithelial ovarian cancer. *Med Oncol* 2010;
 27: 1246-1253.

- 13. Nieto MA, Huang RY, Jackson RA, et al. Emt: 2016. Cell 2016; 166: 21-45.
- 14. Su S, Liu Q, Chen J, *et al.* A positive feedback loop between mesenchymal-like cancer cells and macrophages is essential to breast cancer metastasis. *Cancer Cell* 2014; **25**: 605-620.
- 15. Liu X, Gong H, Huang K. Oncogenic role of kinesin proteins and targeting kinesin therapy. *Cancer Sci* 2013; **104**: 651-656.
- 16. Wiesner C, Faix J, Himmel M, et al. KIF5B and KIF3A/KIF3B kinesins drive MT1-MMP surface exposure, CD44 shedding, and extracellular matrix degradation in primary macrophages. Blood 2010; **116**: 1559-1569.
- 17. Lamouille S, Derynck R. Cell size and invasion in TGF-beta-induced epithelial to mesenchymal transition is regulated by activation of the mTOR pathway. *J Cell Biol* 2007; **178**: 437-451.
- 18. Wei W, Giulia F, Luffer S, *et al*. How can molecular abnormalities influence our clinical approach. *Ann Oncol* 2017; **28**: viii16-viii24.
- 19. Rothenberger NJ, Somasundaram A, Stabile LP. The Role of the Estrogen Pathway in the Tumor Microenvironment. *Int J Mol Sci* 2018; **19**.
- 20. Svensson S, Abrahamsson A, Rodriguez GV, et al. CCL2 and CCL5 Are Novel

 Therapeutic Targets for Estrogen-Dependent Breast Cancer. Clin Cancer Res

 2015; 21: 3794-3805.

- 21. Ning C, Xie B, Zhang L, et al. Infiltrating Macrophages Induce ERalpha Expression through an IL17A-mediated Epigenetic Mechanism to Sensitize Endometrial Cancer Cells to Estrogen. Cancer Res 2016; 76: 1354-1366.
- 22. Zhou Z, Lu ZR. Molecular imaging of the tumor microenvironment. *Adv Drug Deliv Rev* 2017; **113**: 24-48.
- 23. Dun EC, Hanley K, Wieser F, et al. Infiltration of tumor-associated macrophages is increased in the epithelial and stromal compartments of endometrial carcinomas. *Int J Gynecol Pathol* 2013; **32**: 576-584.
- 24. Pena CG, Nakada Y, Saatcioglu HD, *et al.* LKB1 loss promotes endometrial cancer progression via CCL2-dependent macrophage recruitment. *J Clin Invest* 2015; **125**: 4063-4076.
- 25. Kubler K, Ayub TH, Weber SK, et al. Prognostic significance of tumor-associated macrophages in endometrial adenocarcinoma. Gynecol Oncol 2014; 135: 176-183.
- 26. Jarzabek K, Koda M, Walentowicz-Sadlecka M, *et al.* Altered expression of ERs, aromatase, and COX2 connected to estrogen action in type 1 endometrial cancer biology. *Tumour Biol* 2013; **34**: 4007-4016.
- 27. Knapp P, Chabowski A, Blachnio-Zabielska A, *et al.* Expression of estrogen receptors (alpha, beta), cyclooxygenase-2 and aromatase in normal

endometrium and endometrioid cancer of uterus. *Adv Med Sci* 2013; **58**: 96-103.

- 28. Backes FJ, Walker CJ, Goodfellow PJ, *et al.* Estrogen receptor-alpha as a predictive biomarker in endometrioid endometrial cancer. *Gynecol Oncol* 2016; **141**: 312-317.
- 29. Ciucci A, Zannoni GF, Buttarelli M, *et al.* Multiple direct and indirect mechanisms drive estrogen-induced tumor growth in high grade serous ovarian cancers. *Oncotarget* 2016; **7**: 8155-8171.
- 30. Stabile LP, Rothstein ME, Cunningham DE, et al. Prevention of tobacco carcinogen-induced lung cancer in female mice using antiestrogens.

 Carcinogenesis 2012; 33: 2181-2189.
- 31. Iyer V, Klebba I, McCready J, et al. Estrogen promotes ER-negative tumor growth and angiogenesis through mobilization of bone marrow-derived monocytes. Cancer Res 2012; 72: 2705-2713.
- 32. Khan KN, Masuzaki H, Fujishita A, *et al.* Estrogen and progesterone receptor expression in macrophages and regulation of hepatocyte growth factor by ovarian steroids in women with endometriosis. *Hum Reprod* 2005; **20**: 2004-2013.

- 33. Campbell L, Emmerson E, Williams H, et al. Estrogen receptor-alpha promotes alternative macrophage activation during cutaneous repair. J Invest Dermatol 2014; 134: 2447-2457.
- 34. Kramer PR, Wray S. 17-Beta-estradiol regulates expression of genes that function in macrophage activation and cholesterol homeostasis. *The Journal of steroid biochemistry and molecular biology* 2002; **81**: 203-216.
- 35. Ngambenjawong C, Gustafson HH, Pun SH. Progress in tumor-associated macrophage (TAM)-targeted therapeutics. *Adv Drug Deliv Rev* 2017; **114**: 206-221.
- 36. Bingle L, Brown NJ, Lewis CE. The role of tumour-associated macrophages in tumour progression: implications for new anticancer therapies. *The Journal of pathology* 2002; **196**: 254-265.
- 37. Yeh CR, Hsu I, Song W, et al. Fibroblast ERalpha promotes bladder cancer invasion via increasing the CCL1 and IL-6 signals in the tumor microenvironment. American journal of cancer research 2015; 5: 1146-1157.
- 38. Leung SY, Yuen ST, Chu KM, *et al.* Expression profiling identifies chemokine (C-C motif) ligand 18 as an independent prognostic indicator in gastric cancer. *Gastroenterology* 2004; **127**: 457-469.

- 39. Duan H, Zhang X, Wang FX, et al. KIF-2C expression is correlated with poor prognosis of operable esophageal squamous cell carcinoma male patients.

 Oncotarget 2016; 7: 80493-80507.
- 40. Zaganjor E, Osborne JK, Weil LM, *et al.* Ras regulates kinesin 13 family members to control cell migration pathways in transformed human bronchial epithelial cells. *Oncogene* 2014; **33**: 5457-5466.
- 41. Wang H, Liang X, Li M, *et al.* Chemokine (CC motif) ligand 18 upregulates Slug expression to promote stem-cell like features by activating the mammalian target of rapamycin pathway in oral squamous cell carcinoma. *Cancer Sci* 2017; **108**: 1584-1593.
- 42. Maru S, Ishigaki Y, Shinohara N, *et al.* Inhibition of mTORC2 but not mTORC1 up-regulates E-cadherin expression and inhibits cell motility by blocking HIF-2alpha expression in human renal cell carcinoma. *J Urol* 2013; **189**: 1921-1929.
- 43. Hsieh AC, Liu Y, Edlind MP, *et al.* The translational landscape of mTOR signalling steers cancer initiation and metastasis. *Nature* 2012; **485**: 55-61.
- 44. Ohno S, Ohno Y, Suzuki N, *et al.* Correlation of histological localization of tumor-associated macrophages with clinicopathological features in endometrial cancer. *Anticancer Res* 2004; **24**: 3335-3342.

- 45. Wang H, Shao Q, Sun J, *et al.* Interactions between colon cancer cells and tumor-infiltrated macrophages depending on cancer cell-derived colony stimulating factor 1. *Oncoimmunology* 2016; **5**: e1122157.
- 46. Zhao P, Gao D, Wang Q, et al. Response gene to complement 32 (RGC-32) expression on M2-polarized and tumor-associated macrophages is M-CSF-dependent and enhanced by tumor-derived IL-4. Cell Mol Immunol 2015; 12: 692-699.
- 47. Lombardi AP, Pisolato R, Vicente CM, *et al.* Estrogen receptor beta (ERbeta) mediates expression of beta-catenin and proliferation in prostate cancer cell line PC-3. *Mol Cell Endocrinol* 2016; **430**: 12-24.
- 48. Konen J, Wilkinson S, Lee B, *et al.* LKB1 kinase-dependent and -independent defects disrupt polarity and adhesion signaling to drive collagen remodeling during invasion. *Mol Biol Cell* 2016; **27**: 1069-1084.

Table1. The correlation between tumoral stroma CD68 expression and clinicopathological parameters.

Parameter	N	CD68 expression of tumoral stroma		<i>P</i> -value
		high	low	
Age				
<57	38	16	22	0.876
≥57	47	19	28	
Tumor size(cm)				
<3.5	38	15	23	0.774
≥3.5	47	20	27	
Lymph Node Metastasis				
N0	65	24	41	P < 0.001
N1-2	20	18	2	
Distal Metastasis				
0	72	30	42	0.763
1	13	6	7	
FIGO stage				
I - II	55	22	33	0.040
III-IV	30	19	11	
Differentiation				
poorly differentiated	26	12	14	0.952
moderately differentiated	48	17	31	
Well differentiated	11	6	5	

Table2. The correlation between KIF5B expression and clinicopathological parameter.

Parameter	N	KIF5B expression of tumor cell		<i>P</i> -value
		_		
		high	low	
Age				
<57	38	22	16	0.812
≥57	47	26	21	
Tumor size(cm)				
<3.5	38	20	18	0.735
≥3.5	47	23	24	
Lymph Node				
N0	65	30	35	0.062
N1-2	20	14	6	
Distal Metastasis				
0	72	40	32	0.689
1	13	8	5	
FIGO stage				
I - II	55	14	41	0.002
III-IV	30	18	12	
Differentiation				
poorly differentiated	26	20	6	0.964
moderately	48	34	14	
Well differentiated	11	9	2	

Figure legends

Figure 1. The expression of CD68 and ERα in endometrial cancer. (a) The number of CD68⁺ macrophages in 85 tumoral tissue and 85 normal tissue. Each symbol represents one tissue sample (mean+SEM, Mann-Whitney *U*-test) (b) Representative immunohistochemical staining of CD68 in 85 endometrial cancer specimens (magnification: i, 200x; ii, 200x; iii, 200x). (i) CD68⁺ cells within cancer cell nests. (ii) CD68⁺ cells infiltrated the cancer stroma. (iii) CD68⁺ cells along the invasive margin of the tumor. (c) Mean counts of nest macrophages, stroma macrophages and margin macrophages in 85 endometrial cancer specimens. Each symbol represents one tissue sample (mean+SEM, ANOVA) (d) The expression score of ERα in the epithelium plus stroma compartment in the early stage (stage 1-2) (n=55) and advanced stage (stage 3-4) (n=30) groups of endmetrial cancer specimens. (mean+SEM, Mann-Whitney *U*-test). (e) The percentage of samples with ER⁺CD68⁺ macrophages and ER⁻CD68⁺ macrophages in 85 normal specimens and 85 tumoral specimens, respectively (chi-square test). (f) Representative immunohistochemical staining of CD68 and ERα in two consecutive sections in 85 endometrial cancer specimens (100×; 400×). (g) The percentage of cases with ER⁺CD68⁺ macrophages and ER⁻CD68⁺ macrophages cases in the early stage (n=55) and advanced stage groups (n=30) of endometrial cancer specimens (chi-square test). Scale bar: 20 μ m. *P < 0.05, **P < 0.050.01, ***P < 0.001.

This article is protected by copyright. All rights reserved.

Figure 2. ERα agonist-treated M2 cells induced EMT of Ishikawa cells by CCL18 secretion. (a) Transwell chamber assay of Ishikawa cells incubated in CM from 10 nM PPT or MPP treated-M2 cells with or without 10 µg mL⁻¹ anti-CCL18 antibody for 12 h. (b) Analysis of the mean counts of migrating cells per field (mean+SEM, ANOVA, 3 independent experiments). (c) Wound healing assay of Ishikawa cells treated the same as (a) for 24 h. (d) Quantification of wound recovery (mean+SEM, ANOVA, 3 independent experiments). (e) Typical images of 3D spheroid of Ishikawa cells treated the same as (a) for 72 h. (f) Quantification of the longest invasion distance (fold change) (mean+SEM, ANOVA, 3 independent experiments). (g) Representative confocal images from 3 independent experiments of Ishikawa cells treated the same as (a) for 48 h. (h) Representative western blotting images of EMT markers in Ishikawa cells treated as described above. (j) Bar graphs representing the relative protein expressions (fold change) (mean+SEM, ANOVA, 3 independent experiments). (i) The mRNA level of EMT markers in Ishikawa cells treated as described above (mean+SEM, ANOVA, 3 independent experiments). Scale bar: 20 μ m. *P < 0.05, **P< 0.01, ***P < 0.001.

Figure3. ERα agonist promoted CCL18 secretion in M2 macrophages by activating the ERK1/2 pathway. (a) The mRNA levels of cytokines or chemokines in M2 cells treated with 10 nM PPT with or without MPP. M2 was pretreated with 10 nM MPP for 30 min and then treated with PPT for 24 h. DMSO was used as a control. (mean+SEM,

This article is protected by copyright. All rights reserved.

ANOVA, 3 independent experiments) (b) ELISA was used to detect cytokine or chemokine secretion in the CM from M2 cells treated in the same manner as (a). (mean+SEM, ANOVA, 3 independent experiments). (c) Representative western blot from 3 independent experiments showing the time course of 10 nM PPT-induced ERK 1/2 phosphorylation. M2 was treated with PPT for 0-120 min. (d) Bar graphs representing the relative protein expression (fold change). (mean+SEM, ANOVA). (e) Representative western blot from 3 independent experiments showing PPT-induced phosphorylation of ERK1/2. DMSO was used as a control. (f) Bar graphs representing the relative protein expression (fold change). (mean+SEM, ANOVA). (g) CCL18 secretion in M2 cells treated with 10 nM PPT with or without the ERK inhibitor PD980590. M2 was pretreated with 10 μM PD980590 for 30 min and then treated with 10 nM PPT for 24 h. DMSO was used as a control. (mean+SEM, ANOVA, 3 independent experiments). *P < 0.05, **P < 0.01, ***P < 0.001.

Figure 4. Recombinant CCL18 induced EMT in Ishikawa cells. (**a**) Transwell chamber assay of Ishikawa cells treated with rCCL18 (10 ng mL⁻¹ and 20 ng mL⁻¹) for 12 h. PBS was used as a control. (**b**) Analysis of the mean counts of migrating cells per field (mean+SEM, ANOVA, 3 independent experiments). (**c**) Wound healing assay of Ishikawa cells treated with rCCL18 for 24 h. (**d**) Quantification of wound recovery (mean+SEM, ANOVA, 3 independent experiments). (**e**) Typical images of 3D spheroid of Ishikawa cells treated with rCCL18 for 72 h. (**f**) Quantification of the This article is protected by copyright. All rights reserved.

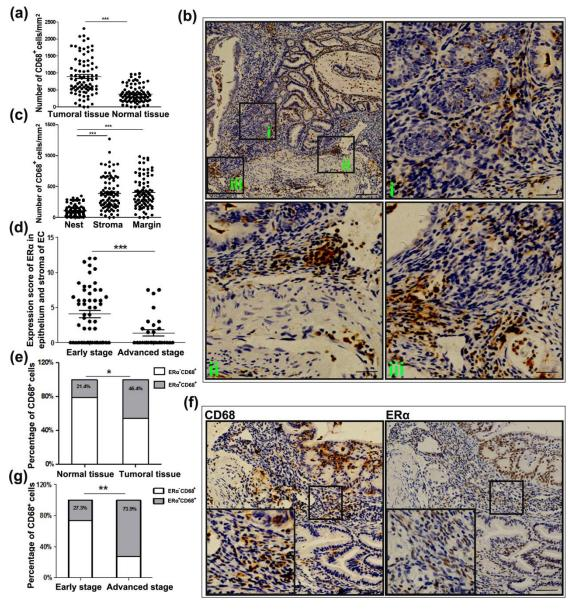
longest invasion distance (fold change) (mean+SEM, ANOVA, 3 independent experiments). (g) Representative confocal images from 3 independent experiments of Ishikawa cells treated with rCCL18 for 48 h. (h) The mRNA level of EMT markers in Ishikawa cells treated as described above (mean+SEM, ANOVA, 3 independent experiments). (i) Representative western blotting images of EMT markers in Ishikawa cells treated as described above. (j) Bar graphs representing the relative protein expressions (fold change) (mean+SEM, ANOVA, 3 independent experiments). Scale bar: $20 \, \mu m$. *P < 0.05, **P < 0.01, ***P < 0.001.

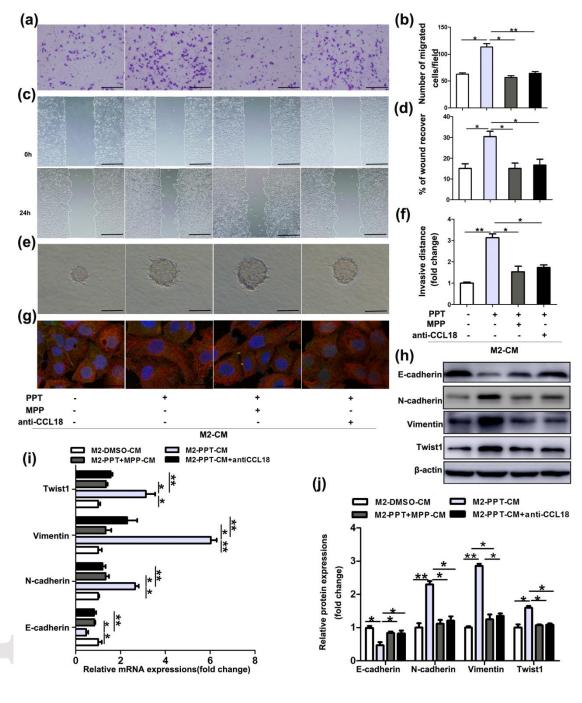
Figure 5. Both rCCL18 and CCL18 from ERα agonist-treated M2 cells induced EMT in Ishikawa cells by KIF5B. (a, b) The mRNA level of KIFs in Ishikawa cells treated with rCCL18 (10 ng mL⁻¹ and 20 ng mL⁻¹) or M2-PPT-CM in the presence or absence of anti-CCL18 at 10 μg mL⁻¹ for 24 h. (mean+SEM, ANOVA, 3 independent experiments). (c, d) Typical images and quantification of Transwell assay in Ishikawa cells transfected with NC or KIF5B-siRNA and then treated with PBS or 20 ng/ml rCCL18 for 12 h. (mean+SEM, ANOVA, 3 independent experiments). (e, f) Typical images and quantification of the Transwell assay in Ishikawa cells transfected with NC or KIF5B-siRNA and then treated with M2-PPT-CM or M2-DMSO-CM for 12 h. (mean+SEM, ANOVA, 3 independent experiments). (g, h) Representative confocal images from 3 independent experiments of Ishikawa cells are displayed. The treatment was the same as above. (i-k) The mRNA and protein level of EMT markers in

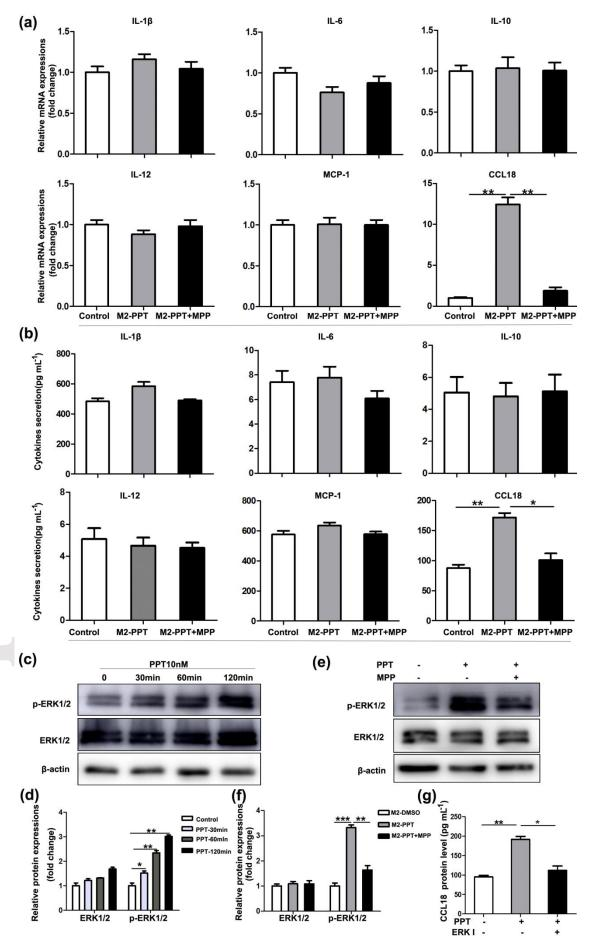
This article is protected by copyright. All rights reserved.

Ishikawa cells transfected with NC or KIF5B-siRNA. (mean+SEM, ANOVA, 3 independent experiments). Scale bar: $20\mu m$. *P < 0.05, **P < 0.01, ***P < 0.001.

Figure6. The expression of KIF5B in endometrial cancer tissue. (a) Representative images of KIF5B expression in 85 normal tissue and 85 endometrial cancer tissue $(100\times; 400\times)$. (b) The percentage of KIF5B^{high} cases and KIF5B^{low} cases and in 85 normal and 85 tumor samples, respectively. (*P < 0.05, chi-square test). (c) The correlation between tumoral CD68⁺ cell numbers and KIF5B expression score in tumor samples. (Spearman's correlation). Scale bar: 20 μm.







This article is protected by copyright. All rights reserved.

